Geophysical Research Letters

RESEARCH LETTER
10.1029/2024GL113080

Response of Australian Summer Monsoon Precipitation to a Strengthening Antarctic Circumpolar Current

Yuhui Han[1], Song Yang[1,2], Peixi Wang[1], Zhenning Li[3], and Xiaoming Hu[1,2]

[1]School of Atmospheric Sciences, Sun Yat-sen University and Southern Marine Science and Engineering Guangdong Laboratory (Zhuhai), Zhuhai, China, [2]Guangdong Province Key Laboratory for Climate Change and Natural Disaster Studies, Zhuhai, China, [3]Division of Environment and Sustainability, The Hong Kong University of Science and Technology, Hong Kong, China

Abstract The Australian summer monsoon (AUSM) is the strongest monsoon in the Southern Hemisphere and it is greatly influenced by the climate conditions in the Indo-Pacific and adjacent regions. Inspite of the substantial studies of the monsoon, the linkage between the AUSM and the high-latitude Southern Ocean climate has not been fully understood. This study investigates how AUSM rainfall is affected by the Antarctic Circumpolar Current (ACC) by simulating scenarios with a closed and an opened Drake Passage with the Community Earth System Model. It is found that AUSM precipitation decreases as a result of reduced local humidity caused by a strengthening ACC. An opened Drake Passage leads to strengthening ACC and Atlantic Meridional Overturning Circulation, which in turn creates an El Niño-like state in the Pacific. This weakens the Walker Circulation, resulting in reduced local moisture, anomalous subsidence over the AUSM region, and a subsequent decrease in monsoon precipitation.

Plain Language Summary Numerous studies have elucidated the intricate linkages between the Australian summer monsoon and various components of the global climate system. However, there remains a notable gap in our understanding of the interaction between the monsoon and the high-latitude climate dynamics. This study investigates the response of monsoon precipitation to perturbations in the Southern Ocean. A strong Antarctic Circumpolar Current is established by removing a land bridge across the Drake Passage in a fully coupled climate model. Australian summer monsoon precipitation decreases as a result of strengthening Antarctic Circumpolar Current, which creates an El Niño-like pattern of sea surface temperature and a weakened Walker Circulation. These features, combined with intensified low-level easterly and southerly winds over the Indo-Pacific Oceans and anomalous subsidence over northern Australia, reduce the moisture and precipitation in situ. This study establishes a crucial linkage between the Australian summer monsoon and Southern Ocean circulation.

Key Points:

- A strengthening Antarctic Circumpolar Current (ACC) is linked to a reduction in Australian summer monsoon (AUSM) precipitation
- A stronger ACC induces more El Niño-like conditions in the Pacific, leading to decreased AUSM precipitation
- Decreased AUSM precipitation is primarily attributed to a loss of local moisture

Supporting Information:

Supporting Information may be found in the online version of this article.

Correspondence to:

X. Hu and S. Yang,
huxm6@mail.sysu.edu.cn;
yangsong3@mail.sysu.edu.cn

Citation:

Han, Y., Yang, S., Wang, P., Li, Z., & Hu, X. (2025). Response of Australian summer monsoon precipitation to a strengthening Antarctic circumpolar current. *Geophysical Research Letters*, *52*, e2024GL113080. https://doi.org/10.1029/2024GL113080

Received 18 OCT 2024
Accepted 31 MAR 2025

1. Introduction

The Australian summer monsoon (AUSM) is the strongest monsoon in the Southern Hemisphere (Geen et al., 2020; Kullgren & Kim, 2006; Troup, 1961), whose precipitation is defined as the mean rainfall from December to February (DJF) in the monsoon region (Kajikawa et al., 2010; Suppiah, 1992), where local summer precipitation exceeds winter precipitation by at least 2 mm/day and accounts for more than 35% of the total annual amount (Zhang & Zhou, 2011; Zhou et al., 2008). Since the 1920s, austral summer rainfall in the Australian monsoon region has increased at a rate of 18 mm/decade (Choi et al., 2016), accelerating to 24 mm/decade after 1950 (Heidemann et al., 2023). Future projections from the Coupled Model Intercomparison Project suggest significant uncertainty in AUSM precipitation under global warming, with possible changes ranging from a 40% increase to a 40% decrease (Brown et al., 2016; Narsey et al., 2020; Zhang & Moise, 2016).

Numerous studies have explored the primary climate drivers and processes influencing the variability in Australian monsoon across various timescales, with a particular focus on the drivers in the Indo-Pacific warm pool. The El Niño-Southern Oscillation (ENSO) exerts a significant influence on the Australian climate, contributing to over 30% of the interannual variability in the monsoon rainfall during austral summer (Catto et al., 2012; Forootan et al., 2016; Sharmila & Hendon, 2020). During La Niña events, northern Australia experiences an earlier monsoon onset, associated more rainfall (Kajikawa et al., 2010). Additionally, the ocean-atmosphere interaction in the Indian Ocean plays an important role in transmitting ENSO signals across northern Australia, which may lead to the monsoon rainfall change as well (Taschetto et al., 2011; Wu &

Kirtman, 2007). Beyond the La Niña impact, Ningaloo Niño events, which are characterized by positive sea surface temperature (SST) and negative sea level pressure anomalies along Australia west coast, can strengthen the trade wind (Zhang & Han, 2018) and influence the large-scale monsoon circulation, resulting in enhanced moisture convergence (Qiao et al., 2002) and increased monsoon rainfall (Li et al., 2013; Zheng et al., 2020).

Both the Interdecadal Pacific Oscillation (IPO; Power et al., 2021) and the Pacific Decadal Oscillation (PDO; Henley et al., 2015; Jaffrés et al., 2018; Power et al., 1999) can regulate the AUSM-ENSO relationship (Meehl & Arblaster, 2011) and the variability in Australian monsoon precipitation during austral summer (Choi et al., 2016; Klingaman et al., 2013; Latif et al., 1997). The negative phases of IPO and PDO lead to a strengthened Pacific Walker Circulation (WC; Sharmila & Hendon, 2020), accompanied by repositioning the ascending branch of the WC and the convection center close to northern Australia (Arblaster et al., 2002). The negative phases are also associated with a southwestward shift of the South Pacific Convergence Zone and a reinforcement of circulation patterns linked to the monsoon rainfall (Folland et al., 2002). Additionally, the enhanced westward winds over the southeastern Indian Ocean during these phases intensify evaporation over northwestern Australia, favoring increased AUSM rainfall (Sharmila & Hendon, 2020).

The climate variability in the Atlantic Ocean also has a significant impact on the Australian monsoon. Warmer tropical SSTs in the Atlantic promote anomalous ascending air over the tropical Atlantic and trigger a mid-latitude Rossby wave train in the southwestern Atlantic, which induces upper-level divergence and leads to wetter conditions over northern Australian (Berry & Reeder, 2015; Lin & Li, 2012). It is also found that the rainfall variation over subtropical eastern Australia has been linked to the North Atlantic Oscillation on decadal time scales, through the oceanic-atmospheric circulation in the Southern Hemisphere (Sun et al., 2015). Moreover, the Atlantic Meridional Overturning Circulation (AMOC), which exhibits weakening signals due to global warming, may also regulate the monsoon by changing the background conditions of SST and circulation in the Indo-Pacific region (Orihuela-Pinto et al., 2022).

Inspite of the studies discussed above, the impact of the Southern Ocean on the Australian monsoon remains less explored. One of the most important circulation systems in the Southern Ocean is the Antarctic Circumpolar Current (ACC). According to the paleoclimate evidence, this oceanic current around the Antarctica reached its present-day strength after its establishment due to the full opening of the Drake Passage (DP) 30 million years ago (Lagabrielle et al., 2009; Lawver & Gahagan, 2003). Since the decadal trend of the circumpolar current around Antarctica was not significant during the 1958–2007 period (Farneti et al., 2015), its effect on global oceanic and atmospheric circulation had been investigated mainly through idealized experiments with different DP states (opened or closed DP) based on various models (Cristini et al., 2012; England et al., 2017; Toggweiler & Bjornsson, 2000; Toggweiler & Samuels, 1995; Yang et al., 2014). The results obtained generally align with observed paleoclimate evidence, indicating that the passage opening contributes to the present-day climate state (Armour et al., 2016; Marshall & Speer, 2012) by establishing the modern-day circumpolar current around Antarctica and meridional overturning circulation, especially the AMOC (Lumpkin & Speer, 2007). Varying climatic mean states formed by the different intensities of oceanic currents around Antarctica may also lead to different SST patterns in tropical regions. For example, an open DP causes cooling in the western Pacific, as shown by the Commonwealth Scientific and Industrial Research Organization Mark version 3L climate model (Hutchinson et al., 2013). Thus, the ACC strengthening, which can influence tropical climate, may change the Australian monsoon precipitation through modulating the tropical circulation. To explore the response of AUSM precipitation to the change in oceanic currents around Antarctica, we analyze two climate states respectively with opened and closed DP using the fully coupled Community Earth System Model (CESM; Hurrell et al., 2013).

This paper is organized as follows. Section 2 describes the two sets of simulations, one with an opened DP and the other with a closed DP. Section 3 provides a brief introduction of the diagnostic analysis of the vertically integrated moisture budget and transport. In Section 4, we examine the impact of the circumpolar current around Antarctica on monsoon precipitation by comparing the results obtained from these two experiments. Finally, a summary and conclusions are given in Section 5.

2. Model and Experiments

In this study, we apply the fully coupled global climate model CESM v1.2.2 (Hurrell et al., 2013). The global climate model has an ocean component whose depth is 5,500 m with 60 vertical layers. The horizontal resolution of the ocean and sea ice components is 1° latitude by 1° longitude. The Community Atmosphere Model version 4

is the atmospheric component of the CESM and its horizontal resolution is 1.9° latitude by 2.5° longitude. The atmospheric component has 26 vertical layers in a σ-P hybrid coordinate system, with a top height extending to 35 km.

This study conducted two fully coupled experiments with the different passage cases: An opened Drake Passage (DPO) and a closed Drake Passage (DPC). Both experiments are based on the B2000 compset in the CESM configuration, which equals the CO_2 concentration of the year 2000. To reach a quasi-equilibrium state, the spin-up period in the DPO case is 249 years. In the DPC case, the oceanic currents around the Antarctic were cut off by a land bridge connecting the Antarctic Peninsula with Cape Horn, South America. The width and height of this land bridge are 500 km and 10 m, respectively. Since a longer timescale is required for the adjustment of oceanic circulation, the DPC case sets a spin-up time of 900 years (Figure S1 in Supporting Information S1). Both experiments are run for 100 years after their quasi-equilibrium state is reached. In these two experiments, the climatological mean values equal to the average of the final 100 years of each simulation. The differences in climatological mean between the two cases (DPO minus DPC) represent the impacts of ACC strengthening on global climate.

Wang et al. (2024) confirmed that the DPO case effectively captured the observed mean climate state globally. Thus, the circumpolar current around Antarctica in the DPO case shown in Figure 1a can represent the observed mean climate state of oceanic currents around Antarctica. Figure 1b reveals the strengthening of this circumpolar current formed by an open DP relative to the oceanic current in the DPC case. In this study, we focus on the AUSM precipitation which is defined as the mean rainfall from December to February (DJF) in the monsoon region, where local summer precipitation exceeds the winter precipitation by more than 2 mm/day and accounts for at least 35% of the total annual amount (Zhang & Zhou, 2011; Zhou et al., 2008). Compared with the counterparts observed from the Global Precipitation Climatology Project v2.3 reanalysis (GPCP) for 2002–2022 (Adler et al., 2018), the climatological mean precipitation from the DPO case has a similar annual average (Figure 1d) and standard deviation (Figure 1e), showing its reliability in repeating the observed climatological precipitation around Australia. The total current transport volume induced by ACC is derived from annual total mass transport vertically integrated through DP (Farneti et al., 2015) in the DPO case and from Ocean Reanalysis System 5 (Zuo et al., 2015) for 2002–2022.

3. Methods

To investigate the impacts of ACC strengthening on monsoon precipitation, we conduct a diagnostic analysis of vertically integrated moisture budget associated with precipitation (as in Li et al., 2020, 2021; Zhao et al., 2019, 2020) by examining the difference in monsoon precipitation between the DPO and DPC cases. The equation for moisture budget can be written as follows:

$$\Delta P = -\Delta < \vec{V}\nabla q > \; - \Delta < q\nabla \cdot \vec{V} > + \Delta E \tag{1}$$

Here, Δ captures the impact of ACC strengthening, denoting the difference between the DPO and DPC cases. P, q, E, and $\vec{V}$ represent precipitation, specific humidity, evaporation, and the wind vectors with both zonal and meridional components, respectively. <> is vertical integration from the surface to 200 hPa and ∇ means the horizontal gradient operator. For the terms on the right-hand side, $-\Delta < \vec{V}\,\nabla\, q>$ is called "moisture loss," denoting the change in moisture advection. $-\Delta < q\,\nabla \cdot \vec{V}>$ is related with ascending motions, designating the change in the total column-integrated convergence of horizontal wind. ΔE indicates evaporation change, which can be neglected as its contribution to rainfall difference is much smaller than the other two terms. Thus, the changes in precipitation due to ACC strengthening can be decomposed into the contributions from both horizontal moisture advection (Figure 1h) and ascending motions (Figure 1i), which will be discussed in detail later.

4. Results

4.1. Impact of the ACC on AUSM Precipitation

Figure 1 shows the differences in climatological mean surface oceanic currents around the Antarctic and AUSM precipitation between the DPO and DPC cases. As shown in Figures 1a and 1b, the surface circumpolar circulation around the Antarctica strengthens in the DPO case compared to the DPC case, which aligns with the

10.1029/2024GL113080

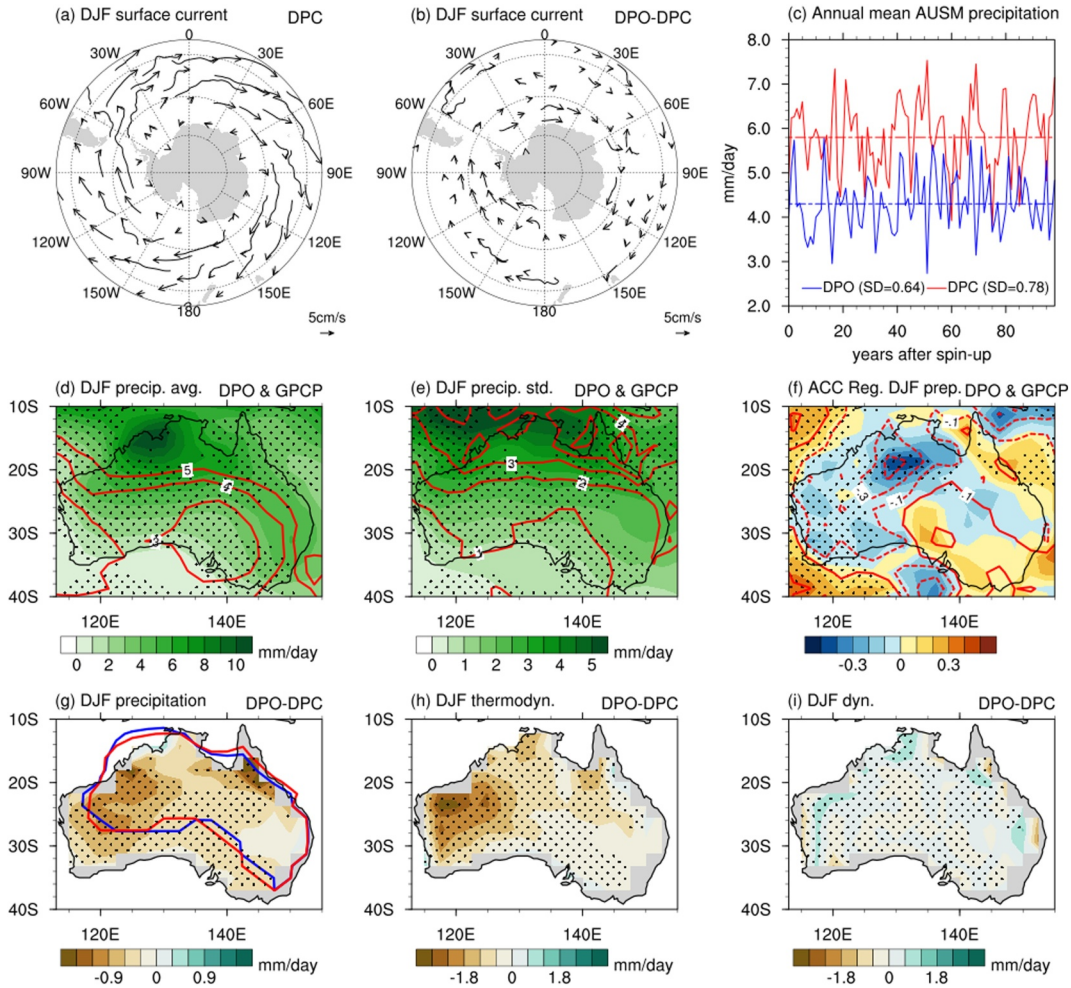

Figure 1. Panels (a, b) show climatological DJF mean (a) average in the DPO case and (b) differences between DPO and DPC cases in the B2000 simulations for surface oceanic currents (cm/s) over 40°-90°S. Panel (c) presents the time series of area-averaged AUSM precipitation (solid lines, mm/day) along with the mean of the 100-year area-averaged precipitation (dashed lines, mm/day) in the DPC (red lines) and DPO cases (blue lines). The standard deviations corresponding to the red and blue lines are 0.78 and 0.64, respectively. Panels (d–f) display (d) DJF mean average (mm/day) and (e) standard deviation of precipitation (mm/day), with (f) correlation coefficients between DJF mean precipitation and total current transport volume induced by ACC in the DPO case (shading) and from reanalysis data (contours; positive and negative are represented by solid and dashed lines, respectively). Panels (g–i) depict climatological DJF mean differences between DPO and DPC cases in the B2000 simulations for (g) precipitation (mm/day), (h) thermodynamic (mm/day), and (i) dynamic contributions (mm/day) to precipitation change. In panel (g), the red (blue) contour indicates AUSM regions in the DPC (DPO) case. Stippling and vectors indicate the significant differences at the 95% confidence level based on the Student's *t*-test.

findings from previous studies (Kennett, 1977, 1978; Lagabrielle et al., 2009; Sijp & England, 2004). Figures 1c and 1g–1i depict the changes in Australian summer precipitation under ACC strengthening. The climatological areal mean daily monsoon precipitation is 4.2 mm/day in the DPO case and 5.8 mm/day in the DPC case (see Figure 1c). This feature indicates that strengthening of ACC leads to a decrease in AUSM precipitation, a relationship that is also evident in the interannual variability observed in both observational data and model simulations (Figure 1f). The decrease in this monsoon precipitation occurs across northeastern and northwestern Australia, with a maximum decrease about 1.5 mm/day, although the overall northern Australian region remains relatively unchanged (Figure 1g). To better understand the mechanism for the reduction in this climatological monsoon precipitation, we apply Equation 1 to decompose the precipitation anomaly into contributions from local moisture loss (Figure 1h) and ascending motions (Figure 1i). The analysis reveals that the change in local moisture loss reduces monsoon precipitation (Figure 1h), while the change in local ascending motions slightly increases monsoon precipitation (Figure 1i). The results of MSE budget analysis (Text S1 in Supporting

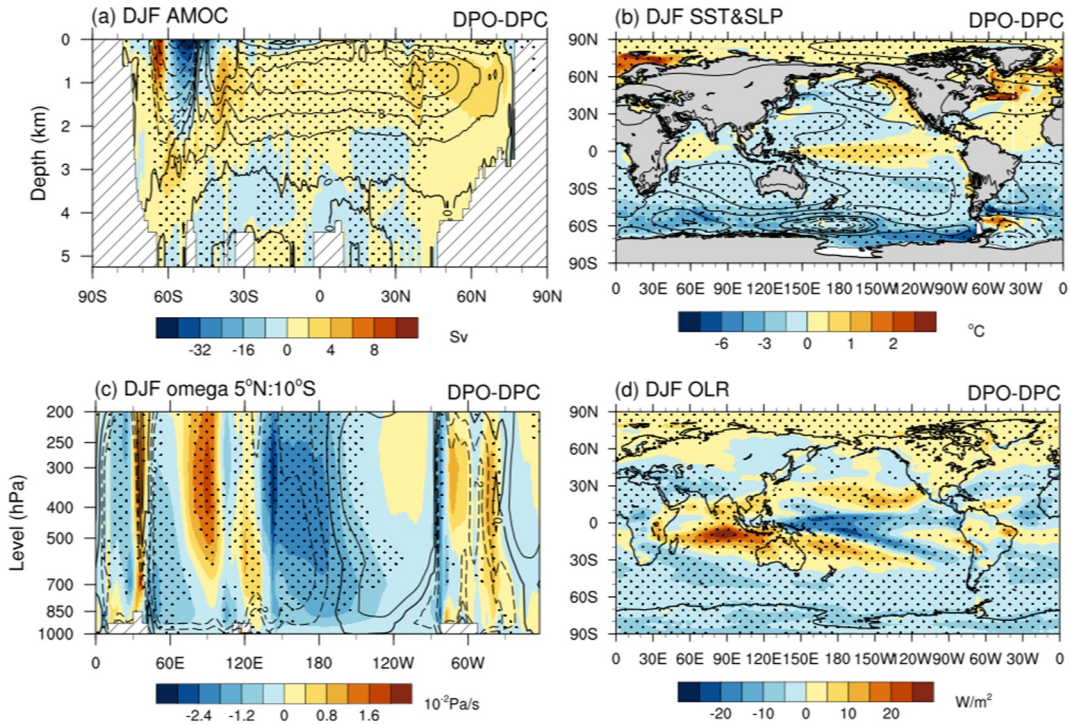

Figure 2. Climatological DJF mean differences between DPO and DPC cases in the B2000 simulations for (a) Atlantic Meridional Overturning Circulation (AMOC) streamfunction (Sv, 1Sv = $10^6 m^3/s$), (b) sea surface temperature (shading, °C) and sea level pressure (contours, hPa), (c) equatorial (5°N–10°S) mean vertical velocity (10^{-2}Pa/s), and (d) outgoing long-wave radiation (W/m^2), with the climatological DJF mean AMOC streamfunction (Sv) and equatorial vertical velocity (10^{-2}Pa/s) in the DPO case overlaid as contours (positive represented by solid lines and negative by dashed lines) shown in panels (a, c). Stippling indicates the significant differences at the 95% confidence level based on the Student's *t*-test.

Information S1), following Sekizawa et al. (2023), also confirm that moisture loss due to horizontal divergence of moisture flux accounts for the largest portion of the decrease in monsoon precipitation (Table S1 in Supporting Information S1). To understand the physical mechanisms for the decrease in monsoon rainfall, we next examine how the ACC strengthening would modulate the large-scale background circulation. These changes in global atmospheric and oceanic circulation patterns could overall explain the decrease in monsoon precipitation.

4.2. Large-Scale Circulation Changes Driven by ACC Strengthening

The main changes in annual mean large-scale oceanic and atmospheric circulation driven by ACC strengthening have been reported in Wang et al. (2024), which include stronger upwelling in the Southern Ocean, a stronger climate-mean AMOC, a colder climate state in the Antarctic, and a warmer climate state in the Arctic. In this study, we specifically focus on the large-scale circulation related to Australian monsoon. Therefore, the changes in large-scale circulation during austral summer are analyzed.

The ACC strengthening enhances the vigorous downwelling in the Southern Ocean and further strengthens the AMOC (Figure 2a). Therefore, the reduced oceanic heat transport in the Atlantic due to the AMOC strengthening, which is found in previous study (Orihuela-Pinto et al., 2022), results in cooling in Antarctica and warming in the Arctic (Figure 2b), particularly in the North Atlantic sector. This asymmetric SST change drives the northward shift and weakening of Hadley Circulation (HC; Figure S2 in Supporting Information S1) and Intertropical Convergence Zone (ITCZ; Figure S3 in Supporting Information S1), with a stronger downdraft between 20 and 30°S and a weakened updraft between 0 and 10°S. In the tropics, the reduced oceanic heat transport causes warming in the Atlantic and the central-eastern Pacific, and cooling in the Indo-Pacific warm pool, leading to a more El Niño-like state in the tropical Pacific. This anomalous SST pattern drives a weakening WC (Figure 2c), with an enhanced anomalous descending branch over the Indian Ocean, the Maritime Continent, and the western Atlantic and a stronger ascending branch over the tropical Pacific. These features are also reflected,

correspondingly, in the change in the cloud cover, as seen from the outgoing long-wave radiation patterns (Figure 2d) with increased values over the anomalous descending branch but decreased values over the anomalous ascending branch. The westward shift of the WC and northward shift of the HC may alter the wind field and moisture patterns over northern Australia, further contributing to the decrease in precipitation. Thus, it becomes crucial to investigate how regional atmospheric processes, particularly those directly linked to monsoon dynamics, respond to ACC strengthening and the related large-scale circulation.

4.3. Regional Atmospheric Circulation Changes and Their Contributions to the Decrease in AUSM Precipitation

Given that the changes in large-scale circulation can affect regional atmospheric circulation over northern Australia, we proceed to reveal the direct mechanisms for the decrease in monsoon rainfall during austral summer. Since the change in precipitation is caused by both the thermodynamic and dynamic processes, we examine how the large-scale background conditions modulated by ACC strengthening would lead to local moisture loss and ascending motions (Figure 3), which is relative with thermodynamic and dynamic contributions to the monsoon precipitation change from December to February.

As aforementioned, according to Equation 1, the decrease in monsoon precipitation is primarily driven by local moisture loss, while the changes in vertical motions tend to have a modest positive effect on Australian precipitation during austral summer. Figures 3a–3e show less precipitable water vapor and moisture divergence over the monsoon region resulting from the changes in regional atmospheric circulation due to ACC strengthening. These changes result in a decrease in the moisture, which significantly contributes to the reduction of Australian precipitation from December to February. As shown in Figure 2b, when the DP is open, the strengthening of circumpolar oceanic currents in the Southern Ocean raises the sea level pressure over northern Australia, which drives enhanced low-level divergence of local moisture flux over northeastern and northwestern Australia (Figures 3b and 3c). Meanwhile, moisture flux at 200 hPa shows anomalous convergence over northern Australia (Figure 3d), which is much weaker compared to the enhanced divergence in the lower troposphere. Therefore, these changes in local moisture flux lead to a significant reduction in precipitable water vapor over northeastern and northwestern Australia (Figure 3a) and moisture loss especially in the lower troposphere (Figure 3e). This is consistent with the contribution to Australian precipitation during austral summer from horizontal moisture advection (Figure 1h). Meanwhile, the ACC strengthening forces stronger downdrafts in the upper troposphere and enhanced updrafts in the lower troposphere especially over central and western Australia (Figure 3f). Specifically, the anomalous updrafts in the lower troposphere may be induced by strong tropical convection over the Maritime Continent (Figure S4 in Supporting Information S1), as suggested by Chen et al. (2019). As local specific humidity is mainly concentrated in the lower troposphere, the contribution of vertical motion to monsoon precipitation is dominated by the enhancement of updraft (Figure 3f), resulting in a small increase in monsoon precipitation over northern Australian regions from December to February (Figure 1i).

5. Conclusions

In this study, we explore the relationship between the Australian summer monsoon (AUSM) and the climatic system in the high-latitude Southern Ocean with a particular focus on the impact of the Antarctic Circumpolar Circulation (ACC) on the monsoon. Using the fully-coupled Community Earth System Model and based on the simulations for the Drake Passage opened and closed scenarios, we demonstrate that strengthening of ACC leads to a significant reduction in Australian monsoon precipitation during austral summer, particularly over northeastern and northwestern Australia. To reveal the mechanism driving the reduction in climatological monsoon precipitation over northern Australia, we examine how the strengthening of climatological mean circumpolar oceanic currents in the high-latitude Southern Ocean would modulate the global and regional circulation patterns. Our analysis shows that the precipitation anomaly can be attributed to two key factors: local moisture loss and change in ascending motions.

Figure 4 summarizes the physical mechanisms through which ACC strengthening leads to a decrease in Australian summer monsoon precipitation. The strengthening of circumpolar surface oceanic circulation around the Antarctic and AMOC not only triggers cooling in Antarctica and warming in the Arctic but also induces a more El Niño-like state in the tropical Pacific. This surface temperature anomaly pattern causes the Hadley Circulation to shift northward and weakens the Walker Circulation, with an enhanced anomalous descending

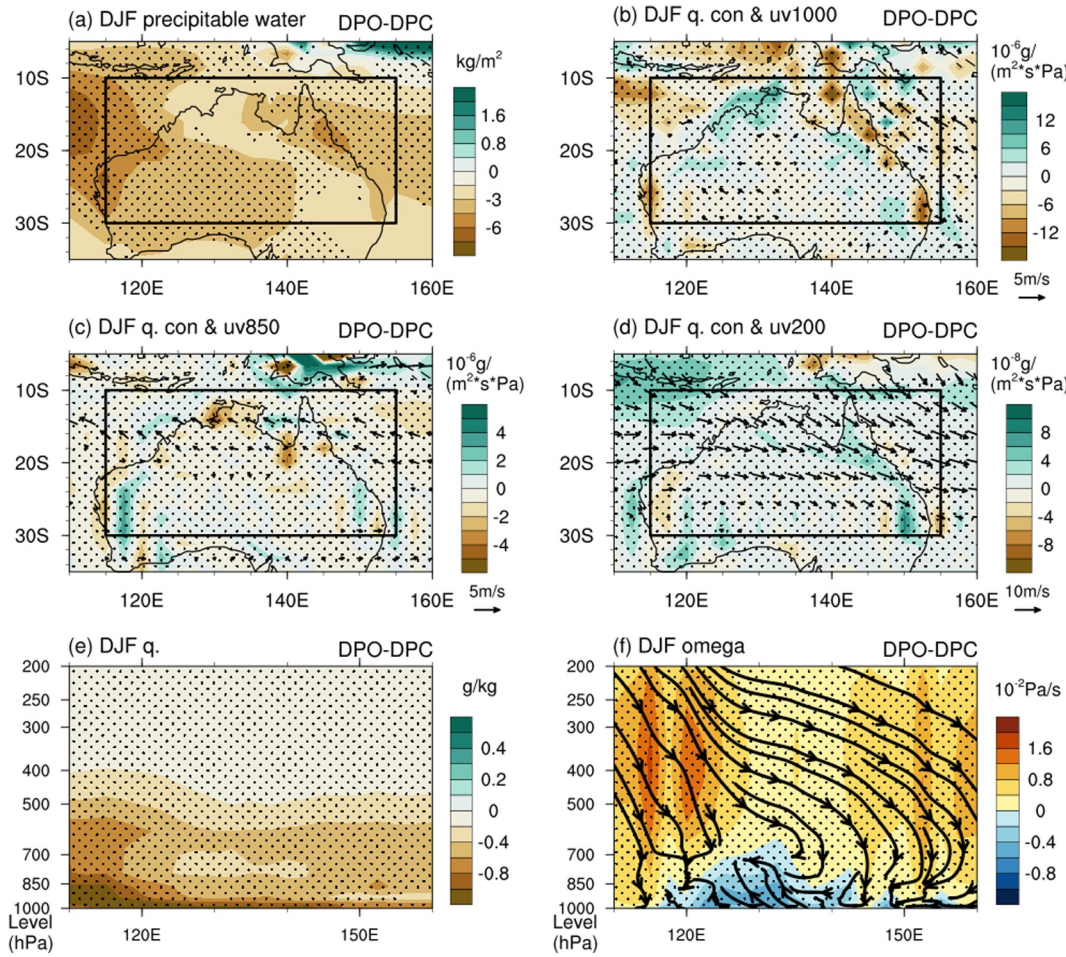

Figure 3. Climatological DJF mean differences between DPO and DPC cases in the B2000 simulations for the (a) total column-integrated water vapor content (kg/m^2) from 200 hPa to 1,000 hPa, (b–d) moisture flux convergence (shading, 10^{-6}g/(m^{2*}s*Pa) and 10^{-8}g/(m^{2*}s*Pa)) and horizontal winds (vectors, m/s) at (b) 1,000 hPa, (c) 850 hPa and (d) 200 hPa, (e) meridional mean specific humidity (g/kg) and (f) vertical velocity (10^{-2}Pa/s) and circulation (streamlines) over the regions (10°–30°S, 115°–155°E) which is shown as black boxes in panels (a–d). Stippling, streamlines and vectors indicate the significant differences at the 95% confidence level based on the Student's *t*-test.

branch over the Maritime Continent and a stronger ascending branch over the tropical Indo-Pacific Oceans. The changes in large-scale atmospheric circulations result in moisture loss and intensified descent in the mid- and upper troposphere, both of which decrease precipitation. Meanwhile, enhanced lower-tropospheric ascent due to these changes in large-scale atmospheric circulations slightly increases precipitation. Overall, these factors lead to a net reduction in AUSM precipitation.

Our findings suggest that a stronger ACC leads to a decrease in AUSM precipitation. This study fills a gap in understanding the link between the changes in Australian monsoon and Southern Hemisphere high-latitude climate. However, there are limitations to this study. For instance, pathways through which the ACC influences AUSM precipitation are not discussed in this study, such as those involving the Indian Ocean (Mbigi & Xiao, 2024) and the jet stream (Martius et al., 2021). Given the lack of an observed significant trend in change of circumpolar surface currents in the high-latitude Southern Ocean (Farneti et al., 2015), our findings are based solely on idealized modeling experiments with limited observational analysis. In future work, we aim to explore the relationship between variability of circumpolar oceanic currents in the Southern Ocean and Australian monsoon rainfall on various timescale using more observational evidence.

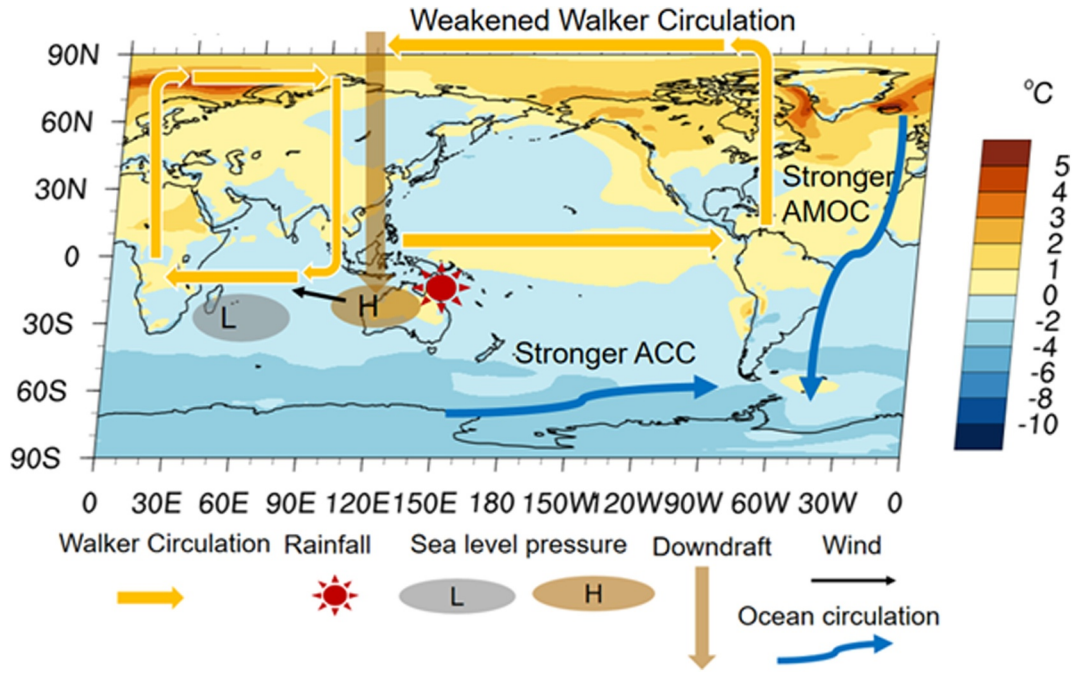

Figure 4. Schematic of the climate response to ACC strengthening. Highlighted are the changes in oceanic and atmospheric circulations, as well as the sea surface temperature (SST) differences (shading) between DPC and DPO cases. ACC strengthening (blue arrow) due to DP opening leads to enhanced Atlantic Meridional Overturning Circulation (AMOC) (blue arrow) and warming in the Arctic and the western Pacific (orange shading). Anomalous heat transport resulting from AMOC strengthening creates a colder Antarctic (blue shading) and a more El Niño-like state in the tropical Pacific. The El Niño-like SST pattern generates weakening Walker Circulation (yellow arrows). The meridional reorganization of atmospheric circulation strengthens sea-level pressure over the South Indian Ocean (gray low-pressure center) and weakens the pressure (brown high-pressure center), with intensifying southeasterly wind over northern Australia (black arrow). The enhanced downdrafts (brown arrow) and moisture loss due to the changes in regional atmospheric processes result in decreased AUSM precipitation (red sun).

Data Availability Statement

The GPCP v2.3 monthly data can be obtained from the NOAA National Centers for Environmental Information (NCEI) as part of the NOAA Climate Data Record (CDR) Program at https://www.ncei.noaa.gov/data/global-precipitation-climatology-project-gpcp-monthly/access. The data used in Figure 1f from Ocean Reanalysis System 5 (Zuo et al., 2015) can be obtained from the Copernicus Climate Change Service (Copernicus Climate Change Service, Climate Data Store, 2021). The ERA5 data for pressure levels (Hersbach et al., 2023a) and single levels (Hersbach et al., 2023b) were used in Table S1 in Supporting Information S1. The Community Earth System Model is publicly available at http://www.cesm.ucar.edu/.

Acknowledgments
The authors thank the editor and reviewers for their valuable comments which helped greatly to improve the manuscript. This study was supported by the National Natural Science Foundation of China (Grants 42088101), and Southern Marine Science and Engineering Guangdong Laboratory (Zhuhai) (Grants SML2021SP302 and 316323005).

References

Adler, R., Sapiano, M., Huffman, G., Wang, J.-J., Gu, G., Bolvin, D., et al. (2018). The Global Precipitation Climatology Project (GPCP) monthly analysis (new version 2.3) and a review of 2017 global precipitation. *Atmosphere*, *9*(4), 138. https://doi.org/10.3390/atmos9040138

Arblaster, J., Meehl, G., & Moore, A. (2002). Interdecadal modulation of Australian rainfall. *Climate Dynamics*, *18*(6), 519–531. https://doi.org/10.1007/s00382-001-0191-y

Armour, K. C., Marshall, J., Scott, J. R., Donohoe, A., & Newsom, E. R. (2016). Southern ocean warming delayed by circumpolar upwelling and equatorward transport. *Nature Geoscience*, *9*(7), 549–554. https://doi.org/10.1038/ngeo2731

Berry, G. J., & Reeder, M. J. (2015). The dynamics of Australian monsoon bursts. *Journal of the Atmospheric Sciences*, *73*(1), 55–69. https://doi.org/10.1175/JAS-D-15-0071.1

Brown, J. R., Moise, A. F., Colman, R., & Zhang, H. (2016). Will a warmer world mean a wetter or drier Australian monsoon? *Journal of Climate*, *29*(12), 4577–4596. https://doi.org/10.1175/JCLI-D-15-0695.1

Catto, J. L., Nicholls, N., & Jakob, C. (2012). North Australian sea surface temperatures and the El Niño–Southern oscillation in observations and models. *Journal of Climate*, *25*(14), 5011–5029. https://doi.org/10.1175/JCLI-D-11-00311.1

Chen, W., Guan, Z., Xu, Q., & Yang, H. (2019). Variation of anomalous convergence around Kalimantan Island in lower troposphere and its role in connecting the East Asian summer monsoon and Australian winter monsoon. *Journal of Geophysical Research: Atmospheres*, *124*(13), 6892–6903. https://doi.org/10.1029/2018JD030215

Choi, K.-S., Kim, H.-D., & Kang, S.-D. (2016). Interdecadal variation of Australian summer monsoon during late 1990s. *International Journal of Climatology*, *36*(4), 1917–1927. https://doi.org/10.1002/joc.4469

Copernicus Climate Change Service, Climate Data Store. (2021). ORAS5 global ocean reanalysis monthly data from 1958 to present [Dataset]. *Copernicus Climate Change Service (C3S) Climate Data Store (CDS)*. https://doi.org/10.24381/cds.67e8eeb7

Cristini, L., Grosfeld, K., Butzin, M., & Lohmann, G. (2012). Influence of the opening of the Drake Passage on the Cenozoic Antarctic Ice Sheet: A modeling approach. *Palaeogeography, Palaeoclimatology, Palaeoecology*, *339–341*, 66–73. https://doi.org/10.1016/j.palaeo.2012.04.023

England, M. H., Hutchinson, D. K., Santoso, A., & Sijp, W. P. (2017). Ice-atmosphere feedbacks dominate the response of the climate system to Drake Passage closure. *Journal of Climate*, *30*(15), 5775–5790. https://doi.org/10.1175/JCLI-D-15-0554.1

Farneti, R., Downes, S. M., Griffies, S. M., Marsland, S. J., Behrens, E., Bentsen, M., et al. (2015). An assessment of Antarctic Circumpolar Current and Southern Ocean meridional overturning circulation during 1958–2007 in a suite of interannual CORE-II simulations. *Ocean Modelling*, *93*, 84–120. https://doi.org/10.1016/j.ocemod.2015.07.009

Folland, C. K., Renwick, J. A., Salinger, M. J., & Mullan, A. B. (2002). Relative influences of the interdecadal Pacific oscillation and ENSO on the South Pacific convergence Zone. *Geophysical Research Letters*, *29*(13), 1643. https://doi.org/10.1029/2001GL014201

Forootan, E. K., Awange, J. L., Schumacher, M., Anyah, R. O., Van Dijk, A. I. J. M., & Kusche, J. (2016). Quantifying the impacts of ENSO and IOD on rain gauge and remotely sensed precipitation products over Australia. *Remote Sensing of Environment*, *172*, 50–66. https://doi.org/10.1016/j.rse.2015.10.027

Geen, R., Bordoni, S., Battisti, D. S., & Hui, K. (2020). Monsoons, ITCZs, and the concept of the global monsoon. *Reviews of Geophysics*, *58*(4), e2020RG000700. https://doi.org/10.1029/2020RG000700

Heidemann, H., Cowan, T., Henley, B. J., Ribbe, J., Freund, M., & Power, S. (2023). Variability and long-term change in Australian monsoon rainfall: A review. *WIREs Climate Change*, *14*(3), e823. https://doi.org/10.1002/wcc.823

Henley, B. J., Gergis, J., Karoly, D. J., Power, S., Kennedy, J., & Folland, C. K. (2015). A tripole index for the interdecadal Pacific oscillation. *Climate Dynamics*, *45*(11–12), 3077–3090. https://doi.org/10.1007/s00382-015-2525-1

Hersbach, H., Bell, B., Berrisford, P., Biavati, G., Horányi, A., Muñoz Sabater, J., et al. (2023a). ERA5 monthly averaged data on pressure levels from 1940 to present [Dataset]. *Copernicus Climate Change Service (C3S) Climate Data Store (CDS)*. https://doi.org/10.24381/cds.6860a573

Hersbach, H., Bell, B., Berrisford, P., Biavati, G., Horányi, A., Muñoz Sabater, J., et al. (2023b). ERA5 monthly averaged data on single levels from 1940 to present [Dataset]. *Copernicus Climate Change Service (C3S) Climate Data Store (CDS)*. https://doi.org/10.24381/cds.f17050d7

Hurrell, J. W., Holland, M. M., Gent, P. R., Ghan, S., Kay, J. E., Kushner, P. J., et al. (2013). The community Earth system model: A framework for collaborative research. *Bulletin of the American Meteorological Society*, *94*(9), 1339–1360. https://doi.org/10.1175/BAMS-D-12-00121.1

Hutchinson, D. K., England, M. H., Santoso, A., & Hogg, A. M. C. (2013). Interhemispheric asymmetry in transient global warming: The role of Drake Passage. *Geophysical Research Letters*, *40*(8), 1587–1593. https://doi.org/10.1002/grl.50341

Jaffrés, J. B. D., Cuff, C., Rasmussen, C., & Hesson, A. S. (2018). Teleconnection of atmospheric and oceanic climate anomalies with Australian weather patterns: A review of data availability. *Earth-Science Reviews*, *176*, 117–146. https://doi.org/10.1016/j.earscirev.2017.08.010

Kajikawa, Y., Wang, B., & Yang, J. (2010). A multi-time scale Australian monsoon index. *International Journal of Climatology*, *30*(8), 1114–1120. https://doi.org/10.1002/joc.1955

Kennett, J. P. (1977). Cenozoic evolution of Antarctic glaciation, the Circum-Antarctic ocean, and their impact on global paleoceanography. *Journal of Geophysical Research*, *82*(27), 3843–3860. https://doi.org/10.1029/JC082i027p03843

Kennett, J. P. (1978). The development of planktonic biogeography in the Southern Ocean during the Cenozoic. *Marine Micropaleontology*, *3*(4), 301–345. https://doi.org/10.1016/0377-8398(78)90017-8

Klingaman, N. P., Woolnough, S. J., & Syktus, J. (2013). On the drivers of inter-annual and decadal rainfall variability in Queensland, Australia. *International Journal of Climatology*, *33*(10), 2413–2430. https://doi.org/10.1002/joc.3593

Kullgren, K., & Kim, K. (2006). Physical mechanisms of the Australian summer monsoon: 1. Seasonal cycle. *Journal of Geophysical Research*, *111*(D20), D20104. https://doi.org/10.1029/2005JD006807

Lagabrielle, Y., Goddéris, Y., Donnadieu, Y., Malavieille, J., & Suarez, M. (2009). The tectonic history of Drake Passage and its possible impacts on global climate. *Earth and Planetary Science Letters*, *279*(3–4), 197–211. https://doi.org/10.1016/j.epsl.2008.12.037

Latif, M., Kleeman, R., & Eckert, C. (1997). Greenhouse warming, decadal variability, or El Niño? An attempt to understand the anomalous 1990s. *Journal of Climate*, *10*(9), 2221–2239. https://doi.org/10.1175/1520-0442(1997)010<2221:GWDVOE>2.0.CO;2

Lawver, L. A., & Gahagan, L. M. (2003). Evolution of Cenozoic seaways in the circum-Antarctic region. *Palaeogeography, Palaeoclimatology, Palaeoecology*, *198*(1–2), 11–37. https://doi.org/10.1016/s0031-0182(03)00392-4

Li, J., Zhao, Y., Chen, D., Kang, Y., & Wang, H. (2021). Future precipitation changes in three key sub-regions of East Asia: The roles of thermodynamics and dynamics. *Climate Dynamics*, *59*(5–6), 1377–1398. https://doi.org/10.1007/s00382-021-06043-w

Li, J., Zhao, Y., & Tang, Z. (2020). Projection of future summer precipitation over the yellow river basin: A moisture budget perspective. *Atmosphere*, *11*(12), 1307. https://doi.org/10.3390/atmos11121307

Li, X. F., Yu, J., & Li, Y. (2013). Recent summer rainfall increases and surface cooling over northern Australia since the late 1970s: A response to warming in the tropical western Pacific. *Journal of Climate*, *26*(18), 7221–7239. https://doi.org/10.1175/JCLI-D-12-00786

Lin, Z., & Li, Y. (2012). Remote influence of the tropical Atlantic on the variability and trend in northwest Australia summer rainfall. *Journal of Climate*, *25*(7), 2408–2420. https://doi.org/10.1175/JCLI-D-11-00020.1

Lumpkin, R., & Speer, K. (2007). Global ocean meridional overturning. *Journal of Physical Oceanography*, *37*(10), 2550–2562. https://doi.org/10.1175/JPO3130.1

Marshall, J., & Speer, K. (2012). Closure of the meridional overturning circulation through Southern Ocean upwelling. *Nature Geoscience*, *5*(3), 171–180. https://doi.org/10.1038/ngeo1391

Martius, O., Wehrli, K., & Rohrer, M. (2021). Local and remote atmospheric responses to soil moisture anomalies in Australia. *Journal of Climate*, *34*, 1–48. https://doi.org/10.1175/JCLI-D-21-0130.1

Mbigi, D., & Xiao, Z. (2024). The southern annular mode: Its influence on interannual variability of rainfall in North Australia. *Climate Dynamics*, *62*(5), 4455–4468. https://doi.org/10.1007/s00382-023-07029-6

Meehl, G. A., & Arblaster, J. M. (2011). Decadal variability of Asian–Australian monsoon–ENSO–TBO relationships. *Journal of Climate*, *24*(18), 4925–4940. https://doi.org/10.1175/2011JCLI4015.1

Narsey, S. Y., Brown, J. R., Colman, R. A., Delage, F., Power, S. B., Moise, A. F., & Zhang, H. (2020). Climate change projections for the Australian monsoon from CMIP6 models. *Geophysical Research Letters*, *47*(13), e2019GL086816. https://doi.org/10.1029/2019GL086816

Orihuela-Pinto, B., England, M. H., & Taschetto, A. S. (2022). Interbasin and interhemispheric impacts of a collapsed Atlantic overturning circulation. *Nature Climate Change*, *12*(6), 558–565. https://doi.org/10.1038/s41558-022-01380-y

Power, S., Casey, T., Folland, C., Colman, A., & Mehta, V. (1999). Inter-decadal modulation of the impact of ENSO on Australia. *Climate Dynamics*, *15*(5), 319–324. https://doi.org/10.1007/s003820050284

Power, S., Lengaigne, M., Capotondi, A., Khodri, M., Vialard, J., Jebri, B., et al. (2021). Decadal climate variability in the tropical Pacific: Characteristics, causes, predictability, and prospects. *Science*, *374*(6563), eaay9165. https://doi.org/10.1126/science.aay9165

Qiao, Y., Luo, H., & Jian, M. (2002). The temporal and spatial characteristics of moisture budgets over Asian and Australian monsoon regions. *Journal of Tropical Meteorology*, *8*(2), 113–120.

Sekizawa, S., Nakamura, H., & Kosaka, Y. (2023). Interannual variability of the Australian summer monsoon sustained through internal processes: Wind-evaporation feedback, dynamical air-sea interaction, and soil moisture memory. *Journal of Climate*, *36*(3), 983–1000. https://doi.org/10.1175/JCLI-D-22-0116.1

Sharmila, S., & Hendon, H. H. (2020). Mechanisms of multiyear variations of Northern Australia wet-season rainfall. *Scientific Reports*, *10*(1), 5086. https://doi.org/10.1038/s41598-020-61482-5

Sijp, W. P., & England, M. H. (2004). Effect of the Drake Passage throughflow on global climate. *Journal of Physical Oceanography*, *34*(5), 1254–1266. https://doi.org/10.1175/1520-0485(2004)034<1254:EOTDPT>2.0.CO;2

Sun, C., Li, J., Feng, J., & Xie, F. (2015). A decadal-scale teleconnection between the North Atlantic Oscillation and subtropical eastern Australian rainfall. *Journal of Climate*, *28*(3), 1074–1092. https://doi.org/10.1175/JCLI-D-14-00372.1

Suppiah, R. (1992). The Australian summer monsoon: A review. *Progress in Physical Geography: Earth and Environment*, *16*(3), 283–318. https://doi.org/10.1177/030913339201600302

Taschetto, A. S., Gupta, A. S., Hendon, H. H., Ummenhofer, C. C., & England, M. H. (2011). The contribution of Indian Ocean sea surface temperature anomalies on Australian summer rainfall during El Niño events. *Journal of Climate*, *24*(14), 3734–3747. https://doi.org/10.1175/2011JCLI3885.1

Toggweiler, J. R., & Bjornsson, H. (2000). Drake passage and palaeoclimate. *Journal of Quaternary Science*, *15*(4), 319–328. https://doi.org/10.1002/1099-1417(200005)15:4<319::AID-JQS545>3.0.CO;2-C

Toggweiler, J. R., & Samuels, B. (1995). Effect of Drake Passage on the global thermohaline circulation. *Deep Sea Research Part I: Oceanographic Research Papers*, *42*(4), 477–500. https://doi.org/10.1016/0967-0637(95)00012-U

Troup, A. J. (1961). Variations in upper tropospheric flow associated with the onset of Australian summer monsoon. *Indian Journal of Meteorology and Geophysics*, *12*(94), 217–230. https://doi.org/10.54302/mausam.v12i2.4184

Wang, P., Yang, S., Li, Z., Song, Z., Li, X., & Hu, X. (2024). Role of the Antarctic circumpolar circulation in current asymmetric Arctic and Antarctic warming. *Geophysical Research Letters*, *51*(13), e2024GL110265. https://doi.org/10.1029/2024GL110265

Wu, R., & Kirtman, B. P. (2007). Roles of the Indian Ocean in the Australian summer monsoon-ENSO relationship. *Journal of Climate*, *20*(18), 4768–4788. https://doi.org/10.1175/JCLI4281.1

Yang, S., Galbraith, E., & Palter, J. (2014). Coupled climate impacts of the Drake passage and the Panama Seaway. *Climate Dynamics*, *43*(1–2), 37–52. https://doi.org/10.1007/s00382-013-1809-6

Zhang, H., & Moise, A. (2016). The Australian summer monsoon in current and future climate. In L. M. V. Carvalho & C. Jones (Eds.), *The monsoons and climate change* (pp. 67–121). Springer.

Zhang, L., & Han, W. (2018). Impact of Ningaloo Niño on tropical Pacific and an interbasin coupling mechanism. *Geophysical Research Letters*, *45*(20), 11300–11309. https://doi.org/10.1029/2018GL078579

Zhang, L., & Zhou, T. (2011). An assessment of monsoon precipitation changes during 1901–2001. *Climate Dynamics*, *37*(1–2), 279–296. https://doi.org/10.1007/s00382-011-0993-5

Zhao, Y., Chen, D., Li, J., Chen, D., Chang, Y., Li, J., & Qin, R. (2020). Enhancement of the summer extreme precipitation over North China by interactions between moisture convergence and topographic settings. *Climate Dynamics*, *54*(5–6), 2713–2730. https://doi.org/10.1007/s00382-020-05139-z

Zhao, Y., Xu, X., Li, J., Zhang, R., Kang, Y., Huang, W., et al. (2019). The large-scale circulation patterns responsible for extreme precipitation over the North China Plain in midsummer. *Journal of Geophysical Research: Atmospheres*, *124*(23), 12794–12809. https://doi.org/10.1029/2019JD030583

Zheng, T., Feng, T., Xu, K., & Cheng, X. (2020). Precipitation and the associated moist static energy budget off western Australia in conjunction with Ningaloo Niño. *Frontiers in Earth Science*, *8*, 597915. https://doi.org/10.3389/feart.2020.597915

Zhou, T., Zhang, L., & Li, H. (2008). Changes in global land monsoon area and total rainfall accumulation over the last half century. *Geophysical Research Letters*, *35*(16), 2008GL034881. https://doi.org/10.1029/2008GL034881

Zuo, H., Balmaseda, M. A., & Mogensen, K. (2015). The ECMWF-MyOcean2 eddy-permitting ocean and sea-ice reanalysis ORAP5. Part 1: Implementation. *ECMWF Tech. Memo.*, *736*. https://doi.org/10.21957/5awbusgo